Neurochemical Research (2019) 44:1079–1089
https://doi.org/10.1007/s11064-019-02739-y

ORIGINAL PAPER

Increase in Glutamatergic Terminals in the Striatum Following Dopamine Depletion in a Rat Model of Parkinson's Disease

Xuefeng Zheng[1] · Ziyun Huang[1] · Yaofeng Zhu[1,2] · Bingbing Liu[3] · Zhi Chen[1] · Tao Chen[1] · Linju Jia[1] · Yanmei Li[1] · Wanlong Lei[1]

Received: 26 October 2018 / Revised: 21 January 2019 / Accepted: 21 January 2019 / Published online: 4 February 2019

Abstract

Dopaminergic neuron degeneration is known to give rise to dendrite injury and spine loss of striatal neurons, however, changes of intrastriatal glutamatergic terminals and their synapses after 6-hydroxydopamine (6OHDA)-induced dopamine (DA)-depletion remains controversial. To confirm the effect of striatal DA-depletion on the morphology and protein levels of corticostriatal and thalamostriatal glutamatergic terminals and synapses, immunohistochemistry, immuno-electron microscope (EM), western blotting techniques were performed on Parkinson's disease rat models in this study. The experimental results of this study showed that: (1) 6OHDA-induced DA-depletion resulted in a remarkable increase of Vesicular glutamate transporter 1 (VGlut1) + and Vesicular glutamate transporter 2 (VGlut2)+ terminal densities at both the light microscope (LM) and EM levels, and VGlut1+ and VGlut2+ terminal sizes were shown to be enlarged by immuno-EM; (2) Striatal DA-depletion resulted in a decrease in both the total and axospinous terminal fractions of VGlut1+ terminals, but the axodendritic terminal fraction was not significantly different from the control group. However, total, axospinous and axodendritic terminal fractions for VGlut2+ terminals declined significantly after striatal DA-depletion. (3) Western blotting data showed that striatal DA-depletion up-regulated the expression levels of the VGlut1 and VGlut2 proteins. These results suggest that 6OHDA-induced DA-depletion affects corticostriatal and thalamostriatal glutamatergic synaptic inputs, which are involved in the pathological process of striatal neuron injury induced by DA-depletion.

Keywords Vesicular glutamate transporter · Parkinson's disease · DA-depletion · Striatum · Rat

Introduction

Striatum is the major input nucleus of the basal ganglia, which is primarily involved in the control and execution of goal-directed behaviors and habits [1, 2]. Dysfunction of the striatum leads to severe neurological and psychiatric disorders, such as Parkinson's disease (PD) and Huntington's disease [3]. The principal neurons of the striatum are medium spiny neurons (MSNs), which occupy 90–95% of total striatal neurons. MSNs can be divided into direct pathway and indirect pathway neurons basing on their marker proteins and projection targets [4–6]. Direct pathway neurons express dopamine 1 receptor (D1) and substance P (SP), and project axons to the substantia nigra pars reticulata (SNr) and internal segment of the globus pallidus (GPi). Indirect pathway neurons express dopamine 2 receptor (D2) and enkephalin (ENK), and project axons to external segment of globus pallidus (GPe) [2, 7, 8]. Striatal-direct and indirect pathway neurons share similar morphology, which have radially projecting dendrites with dense dendritic spines [9, 10]. In rodents, the dendrites of individual MSNs harbor as many as 5000 spines [11]. The MSNs are regulated by DA from the substantia nigra pars compacta (SNc) and by glutamic acid from the cortex and thalamus. Inhibitory dopaminergic inputs generally terminate onto the neck of

Xuefeng Zheng and Ziyun Huang have contributed equally to this article.

✉ Wanlong Lei
leiwl@mail.sysu.edu.cn

[1] Department of Anatomy, Zhongshan School of Medicine, Sun Yat-sen University, Guangzhou, China

[2] Institute of Medicine, College of Medicine, Jishou University, Jishou, China

[3] Department of Anesthesiology, Guangdong Second Provincial General Hospital, Guangzhou, China

spines, while excitatory glutamatergic inputs mainly target the head of the spines [12, 13]. This connection pattern provides an anatomical basis for the close synaptic interactions between glutamatergic and dopaminergic inputs at the level of the spines [14, 15]. These interactions are critical for maintaining functional and structural integrity of striatal neurons [16, 17]. Furthermore, it is generally accepted that VGlut1 and VGlut2 are specific markers that can distinguish between cortical afferents and thalamic afferents of the striatum. Cortical neurons which innervate the striatum express VGlut1. Alternatively, the thalamic afferents are mainly from the Parafascicular nucleus (PFn) of the thalamus, and express VGlut2 [18, 19].

Degeneration of the nigrostriatal dopaminergic pathway is the main pathological feature of PD [20–22]. Striatal DA-depletion induces an imbalance between excitatory and inhibitory afferents to the striatum and leads to complex physiological and morphological changes in the striatum [23–25]. Our previous studies confirmed that DA-depletion could lead to behavior disorders relevant to striatal function accompanied by striatal neuron apoptosis in the striatum of PD rat models [26]. In addition, a number of studies have indicated that DA-depletion can reduce dendrite length and cause severe spine loss in PD patients and PD rats, mice and monkey models [9, 27–30]. However, the fate of the glutamatergic presynaptic terminals on the head of spines is still unclear. Researchers assumed that these terminals might move to an alternative postsynaptic target or degenerate after the spine loss [13]. Immunohistochemical data have indicated that VGlut1+ synapses were either significantly increased or unchanged in the striatum of 1-methyl-4-phenyl-1,2,3,6-tetrahydropyridine (MPTP)-treated monkeys, while the prevalence of VGlut2+ synapses either did not change or decreased after MPTP treatment [31, 32]. Moreover, there were significant PFn neurons loss in monkey PD models and PD patients [33–35], but the remaining PFn neurons were intensely hyperactive and showed a marked increase in the expression level of VGlut2 mRNA [36]. The possibility of PFn neuron loss or morphological changes to thalamostriatal systems in rodent PD models remains controversial [37–39]. Moreover, western blotting and immunoautoradiography results have demonstrated that VGlut1 and VGlut2 expression levels were increased by 24% and 29%, respectively, in the putamen of PD patients [40]. However, other researchers found no significant changes in VGlut1 or VGlut2 expression levels in the striatum of PD rat models [41]. In addition, most previous studies have focused on VGluts+ excitatory synapses which can be recognized by the presence of round vesicles in the terminal and a postsynaptic density (PSD) in the spine or dendrite [24, 31, 40, 42–44]. However, we found that most VGlut1+ and VGlut2+ terminals formed asymmetric synapses with spines or dendrites at the EM level. Furthermore, we observed many terminals with no overt PSD, and these terminals were ignored in previous studies.

Unilateral destruction of the dopaminergic pathway in rat by 6OHDA is a well characterized animal model of PD [45, 46]. With the aid of immunohistochemistry, immuno-EM and western blotting techniques, we investigated the changes in density, size and terminal fraction of VGluts+ terminals and protein expression levels of VGlut1 and VGlut2 in the striatum of rats with 6OHDA-induced DA-depletion. Our data showed that both corticostriatal and thalamostriatal inputs underwent complex morphological changes in rat models of PD.

Materials and Methods

Animals and Groups

All animal experiments were performed according to the National Institutes of Health Guide for the Care and Use of Laboratory Animals conducted and approved by the Animal Care and Use Committee of Sun Yat-sen University. Sixty adult male Sprague-Dawley rats weighing 250–300 g were used in this study, and these rats were housed under a 12 h light/dark cycle with access to food and water. Rats were randomly divided into four groups: normal control group (n = 15), sham-operation group (n = 15), vehicle control group (n = 15), and 6OHDA group (n = 15). In each group, six rats were used for immunohistochemistry, three rats for immune-EM detection and six rats were used for western blotting.

Surgical Operation

The PD rat models used in this study have been described in previous articles [26, 47, 48]. Briefly, 6OHDA (catalog no. H116; Sigma) was unilaterally injected into the right median forebrain bundle (MFB) of rats in the 6OHDA group. Rats were anesthetized with sodium pentobarbital (50 mg/kg, i.p.), and then placed on a Kopf stereotaxic instrument (catalog no. 60191, Stoelting Co.). The skull was exposed (coordinates: ML: − 1.9 mm, AP: − 3.6 mm, DV: − 8.2 mm), and 8 ul 6OHDA (2.5 μg/μl 6OHDA dissolved in 0.9% saline containing 0.01% ascorbic acid as antioxidant) was injected into MFB with a 10 μl Hamilton syringe. Rats in the vehicle control group received an equal volume of 0.9% saline containing 0.01% ascorbic acid injected into the same location. Rats in the sham-operation group had the skull exposed and had a hole drilled in the skull, but no treatment was administered. Rats in the normal control group did not receive any surgery or treatment. During the 2–4 weeks following 6OHDA lesions, rats were subcutaneously injected with apomorphine (APO; catalog no. 2073/50, Tocris) at a dose of

0.25 mg/kg, and the number of 360° contralateral rotations within 30 min were counted. Only rats with a total number of turns over 210 were included for further studies [26]. In addition, immunohistochemical staining of tyrosine hydroxylase (TH) in slices of the striatum and SNc were performed for each rat. Only rat models with more than 90% loss of TH neurons in the SNc and 80% loss of TH fibers in the striatum from the ipsilateral hemisphere were used in the following experiments [26, 46, 49]. All rats qualified for analysis and were sacrificed at 28 days after surgery.

Immunohistochemistry and Immuno-EM

After anesthesia with sodium pentobarbital (50 mg/kg, i.p.), rats used for immunohistochemistry were perfused transcardially with 0.9% saline (400 ml) followed by 400 ml of 4% paraformaldehyde–15% saturated picric acid in 0.1 M phosphate buffer (PB; pH 7.4). Rats used for immune-EM were perfused in the same way, but 0.6% glutaraldehyde was added to the fixative. All brains were quickly removed and immersed in 4% paraformaldehyde–15% saturated picric acid in 0.1 M PB overnight at 4 °C, then sectioned at 50 µm by vibratome (catalog no. VT1200S, Leica). Sections were pretreated with 1% sodium borohydride in 0.1 M PB for 30 min followed by 0.3% Hydrogen proxide (H_2O_2) in 0.1 M PB (pH 7.4) for 30 min, then incubated for 48 h at 4 °C in primary antibody: guinea pig anti-VGlut1 (1:1000, catalog no. AB5905, Millipore) or guinea pig anti-VGlut2 (1:2000, catalog no. AB2251-I, Millipore) with 0.1 M PB containing 1% bovine serum albumin. Sections were subsequently rinsed and incubated with secondary antibodies for 3 h at room temperature: biotinylated donkey–anti-guinea pig IgG (1:100, catalog no. 706-065-148, Jackson). Sections were rinsed three times in 0.1 M PB, incubated with avidin–biotin solution (1:200, catalog no. PK-6100, VECTOR labs), then rinsed six times in 0.1 M PB. After the PB rinses, the sections were immersed in 0.05% DAB (catalog no. D5637, Sigma) in 0.1 M PB for 15 min. H_2O_2 was added into the solution with a final concentration of 0.01%, and the sections were incubated in this solution for an additional 5 min. Sections were subsequently washed six times in 0.1 M PB for. Sections to be viewed by LM were mounted onto gelatin-coated slides, air dried, dehydrated with an alcohol gradient, cleared with xylene and covered with neutral balsam.

After DAB visualization, sections for EM were rinsed in 0.1 M sodium cacodylate buffer (catalog no. 6131-99-3, Xiya reagent), then postfixed for 1 h in 2% osmium tetroxide (OsO_4; catalog no. 18456, PELCO) in 0.1 M sodium cacodylate buffer. Sections were then dehydrated in a graded series of ethyl alcohols, impregnated with 1% uranyl acetate in 100% alcohol and flat embedded in EPON 812 resin (catalog no. 18010, PELCO). Ultrathin sections were cut with an ultramicrotome (catalog no. EM UC6, Leica). The sections were mounted on mesh grids, stained with 0.4% lead citrate and 4.0% uranyl acetate, and finally viewed and photographed with an transmission electron microscope (TEM; catalog no. Tecnai G^2 Spirit Twin, FEI company).

Western Blotting

Western blotting was carried out to detect the expression levels of VGlut1 and VGlut2. Rats were killed by decapitation after deep anesthesia with sodium pentobarbital (50 mg/kg, i.p.), and the striatum of each rat was extracted and homogenized. Samples were separated by a 12% SDS-PAGE gel and transferred to PVDF membranes (catalog no. IPVH00010, Millipore). After blocking with 5% nonfat dry milk for 2 h at room temperature, the membranes were incubated overnight at 4 °C with primary antibodies: guinea pig anti-VGlut1 (1:1000, catalog no. AB5905, Millipore), guinea pig anti-VGlut2 (1:1000, catalog no. AB2251-I, Millipore) and rabbit-anti-GAPDH (1:1000, catalog no. mAB5174). The membranes were incubated with horseradish peroxidase (HRP) conjugated goat–anti-guinea pig IgG (1:5000, catalog no. AP97155, Abcam) and HRP conjugated goat anti-rabbit IgG antibody for 2 h at room temperature. The immunoreactive bands were visualized with chemiluminescent HRP substrate (catalog no. WBKLs0500, Millipore).

Data Collection and Statistical Analysis

According to the atlas of Paxinos and Watson [50], the sections were approximately taken from the interaural plane levels (from 10.70 to 8.74 mm). We focused on the dorsolateral striatum region, which is closely related to the motor symptoms of PD [16, 51]. For each striatal level, adjacent sections were immunolabeled with VGlut1 and VGlut2 antibodies; LM observation showed that VGlut1+ and VGlut2+ terminals were uniformly distributed throughout the striatum. The investigators were blinded to measure the different experimental groups. Counting methods for density of terminals were performed as previously described [47, 52, 53]. Briefly, the density of VGlut1+ or VGlut2+ terminals were counted in five randomly selected squares with their sides as 100 µm.

For immuno-EM data, analysis and quantification were carried out on random fields of digital EM images. To only use tissue with adequate antibody penetration, the EM analyses were restricted to ultrathin sections from the most superficial sections of blocks. The size of terminals was determined by measuring them at their widest diameter parallel to and 0.1 µm before the presynaptic membrane. VGlut1+ and VGlut2+ terminals were recognized by immunoreactivity products and densely packed with round, electron-lucent vesicles. Spines were identifiable by their small size, continuity with dendrites, prominent PSD and/or the presence

of the spine apparatus [54–56]. Dendrites were identifiable by their size, oval or elongate shape, and the presence of microtubules and mitochondria. The numbers of VGlut1+ and VGlut2+ terminals (per 100 μm^2) were counted as the density of terminals. VGlut1+ or VGlut2+ immunolabeled terminals targeted on spines or dendrites were counted to ascertain the densities of axospinous and axodendritic synapses. The analysis was performed based on 45 EM images per animal for each marker. For detailed count methods please refer to our previous papers [54–56].

SPSS 20.0 software was used for all statistical analyses. All experimental data were expressed as the mean ± standard deviation. For comparison between two groups, two-way analysis of variance (ANOVA) was used. In all cases, $P < 0.05$ was considered to be statistically significant.

Results

The experimental data showed that there were no significant differences among the normal control group, the sham-operation group, and the vehicle control group (data not shown). To make the following report clear and concise, the data are presented in the text consist of only the control group and the 6OHDA group unless otherwise indicated.

Effects of Striatal DA-Depletion on VGlut1+ and VGlut2+ Terminals Morphology

Previous studies had confirmed that corticostriatal and thalamostriatal terminals could be specifically immunolabeled by VGlut1 and VGlut2, respectively [40, 57]. Immunolabeling of VGlut1 and VGlut2 revealed numerous immunolabeled terminals that were uniformly distributed in the dorsolateral striatum of the control and the 6OHDA groups at the LM level (Fig. 1a, a′, b, b′). Statistical data showed that VGlut1+ terminals in the 6OHDA group (23.36 ± 2.62/100 μm^2) were denser than the control group (19.56 ± 2.01/100 μm^2; $P < 0.05$). Similarly, 6OHDA-induced DA-depletion brought about a remarkable increase of VGlut2+ terminal density (14.18 ± 1.46/100 μm^2) compared to the control group (10.95 ± 1.55/100 μm^2; $P < 0.05$).

EM was applied to accurately investigate ultrastructural features of VGlut1+ and VGlut2+ terminals. VGlut1+ and VGlut2+ terminals tended to be round and uniformly distributed across the dorsolateral striatum, which were densely packed with round, electron-lucent vesicles (Fig. 1c, c′, d, d′). Most VGlut1+ and VGlut2+ terminals formed asymmetric synapses with thicker PSD, and three targeting types of terminals were observed at EM level: (1) VGluts+ terminals targeting spines of striatal neurons forming axospinous synapses; (2) VGluts+ terminals connecting with dendrites of striatal neurons forming axodendritic synapses; (3) VGluts+ terminals without synapse formation (Figs. 2, 3).

To detect and compare the terminal density between the control and the 6OHDA groups, all VGluts+ terminals were counted and their sizes were measure regardless of whether they formed synapses with spines or dendrites (Fig. 1 c, c′, d, d′). Present EM data, in line with LM observation, showed a significant increase in VGlut1+ terminal density in the 6OHDA group (16.49 ± 1.24/100 μm^2) compared with the control group (14.87 ± 1.05/100 μm^2, $P < 0.05$; Fig. 4a), and the density of VGlut2+ terminals also increased in the 6OHDA group (11.77 ± 1.20/100 μm^2) in comparison with the control group (9.76 ± 0.87/100 μm^2, $P < 0.05$; Fig. 4a).

Furthermore, the sizes of VGlut1+ and VGlut2+ terminals were measured in both control and 6OHDA groups. Compared with the control group (0.69 ± 0.28 μm), VGlut1+ terminals were larger in the 6OHDA group (0.87 ± 0.28 μm, $P < 0.05$; Fig. 4b). Similarly, VGlut2+ terminals were smaller in the control group (0.59 ± 0.16 μm) in comparison with the 6OHDA group (0.77 ± 0.22 μm, $P < 0.05$; Fig. 4b).

Morphological Changes of VGlut1+ and VGlut2+ Synapse Connection Patterns After Striatal DA-Depletion

To assess the effect of striatal DA-depletion on glutamatergic synapse connection patterns, we calculated terminal fraction as the ratio of each type of terminal to the total number of terminals (Figs. 2, 3). Even though the densities of VGluts+ terminals were increased with striatal DA-depletion, present data showed that the VGlut1+ total terminal fraction, which include the axospinous and axodendritic terminal fraction, was lower in the 6OHDA group (73.97 ± 4.25%) than the control group (91.26 ± 5.87%, $P < 0.05$; Fig. 4c). Moreover, the axospinous terminal fraction for VGlut1+ terminals was significant reduced in the 6OHDA group (65.98 ± 4.23%) compared to the control group (82.59 ± 6.31%, $P < 0.05$; Fig. 4c), but the terminal fraction was not significantly different between the 6OHDA group (8.24 ± 0.39%) and the control group (8.33 ± 0.41%, $P > 0.05$; Figs. 2, 4c). Similarly, the total terminal fraction for VGlut2+ terminals in the 6OHDA group (69.70 ± 6.31%) significantly declined compared to the control group (92.87 ± 5.34%, $P < 0.05$; Fig. 4d). Additionally, DA-depletion resulted in a lower rate of VGlut2+ axospinous synapses (45.87 ± 5.94%) than its control (65.43 ± 5.54%, $P < 0.05$; Fig. 4d). In contrast with the VGlut1+ terminals, the axodendritic terminal fraction of VGlut2+ terminals decreased significantly in the 6OHDA group (23.80 ± 1.34%) compared to the control group (28.31 ± 0.90%, $P < 0.05$; Figs. 3, 4d).

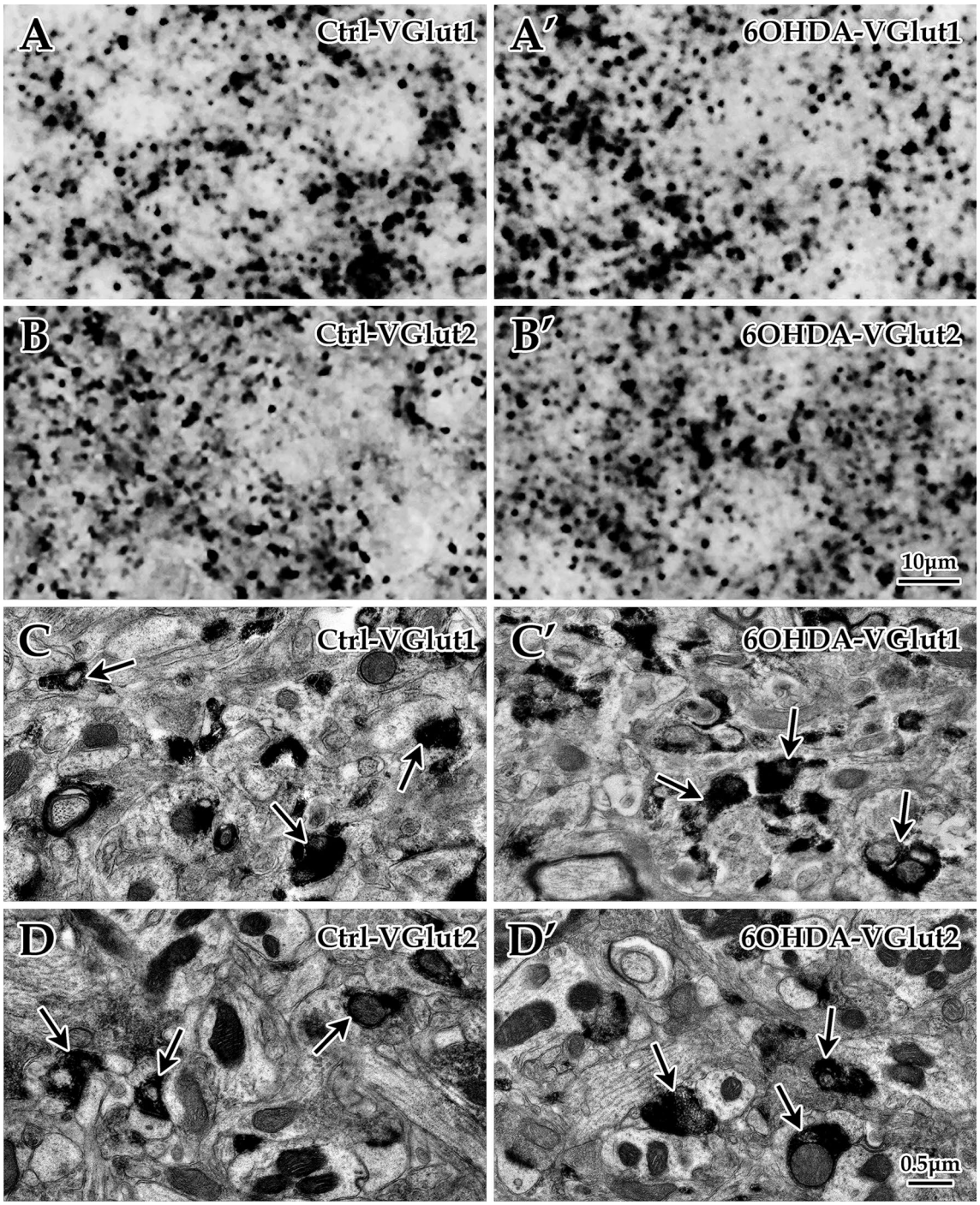

Fig. 1 Morphological changes in VGlut1+ and VGlut2+ terminal densities after striatal DA-depletion. LM (**a, a′, b, b′**) and EM (**c, c′, d, d′**) images for VGlut1+ (**a, a′, c, c′**) and VGlut2+ (**b, b′, d, d′**) reveal terminals in the control group (**a, b, c, d**) and the 6OHDA group (**a′, b′, c′, d′**). Both LM and EM examination showed that the densities of VGlut1+ and VGlut2+ terminals were higher in the 6OHDA group than the control group. The black arrow (→) represents VGluts+ terminals. **a, a′, b, b′** are the same magnification and the scale bar = 10 μm. **c, c′, d, d′** are the same magnification and scale bar = 0.5 μm

Characteristic Responses of VGlut1 and VGlut2 Protein Expression Levels to Striatal DA-Depletion

In accordance with the morphological changes of VGlut1+ and VGlut2+ terminals, western blotting data showed that striatal DA-depletion distinctly up-regulated the expression level of VGlut1 (1.22 ± 0.10) compared to the control group (1.00 ± 0.11, $P < 0.05$; Fig. 5). Further, the expression level of VGlut2 protein was higher in the

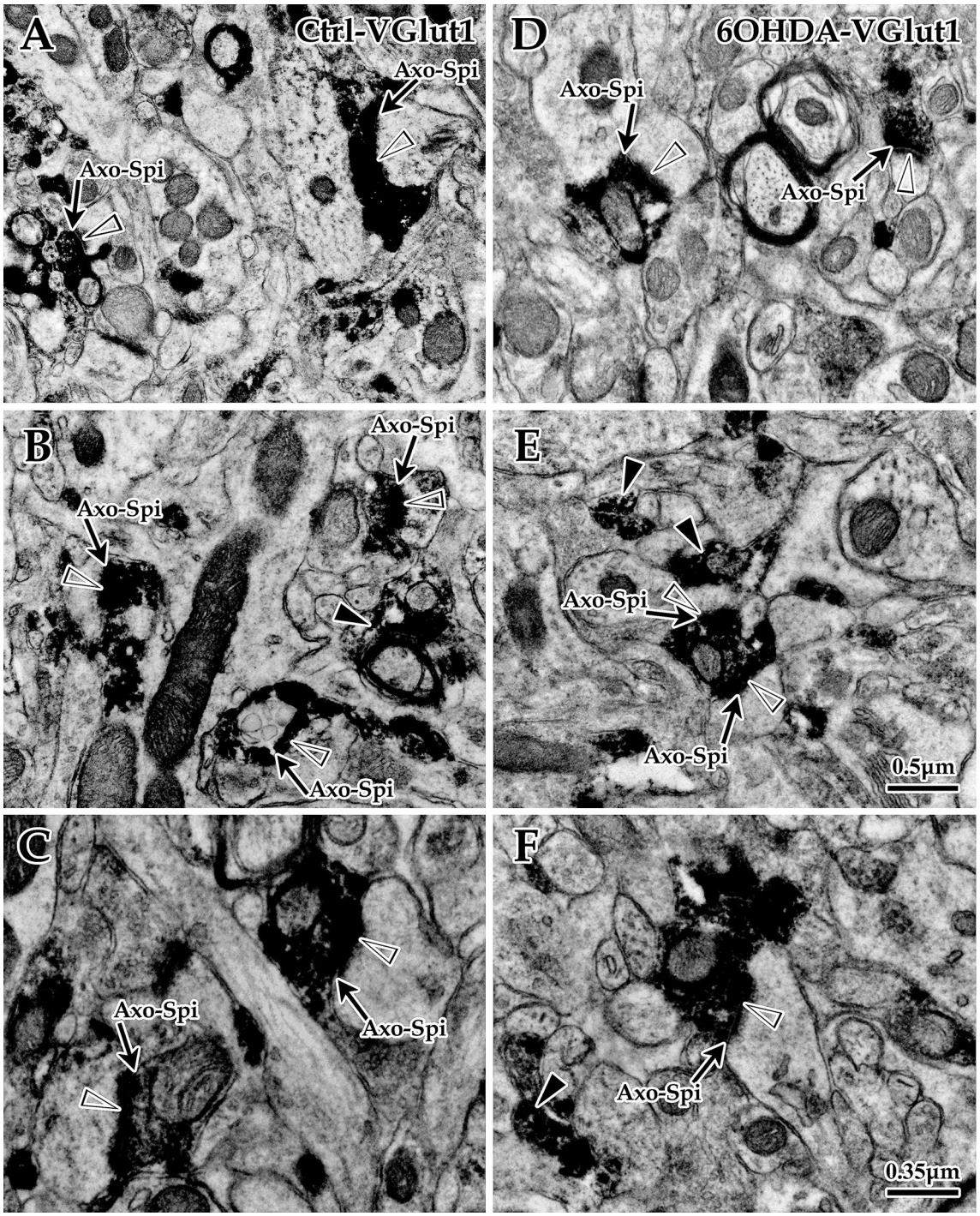

Fig. 2 Immuno-EM exploration for morphological changes in the intrastriatal VGlut1+ synapses after 6OHDA-induced DA-depletion. VGlut1+ terminals are shown in the control group (**a**–**c**) and the 6OHDA group (**d**–**f**). The black arrow (→) represents VGlut1 immunolabeled excitatory synapses. White arrowheads (open triangle) point to PSD of asymmetric synapses. The black arrowheads (closed triangle) indicate VGlut1+ terminals without synapse formation. *Axo-Spi* axospinous synapses, *Axo-Den* axodendritic synapses. **a, b, d, e** were the same magnification and scale bar = 0.5 μm. **c, f** were the same magnification and scale bar = 0.5 μm

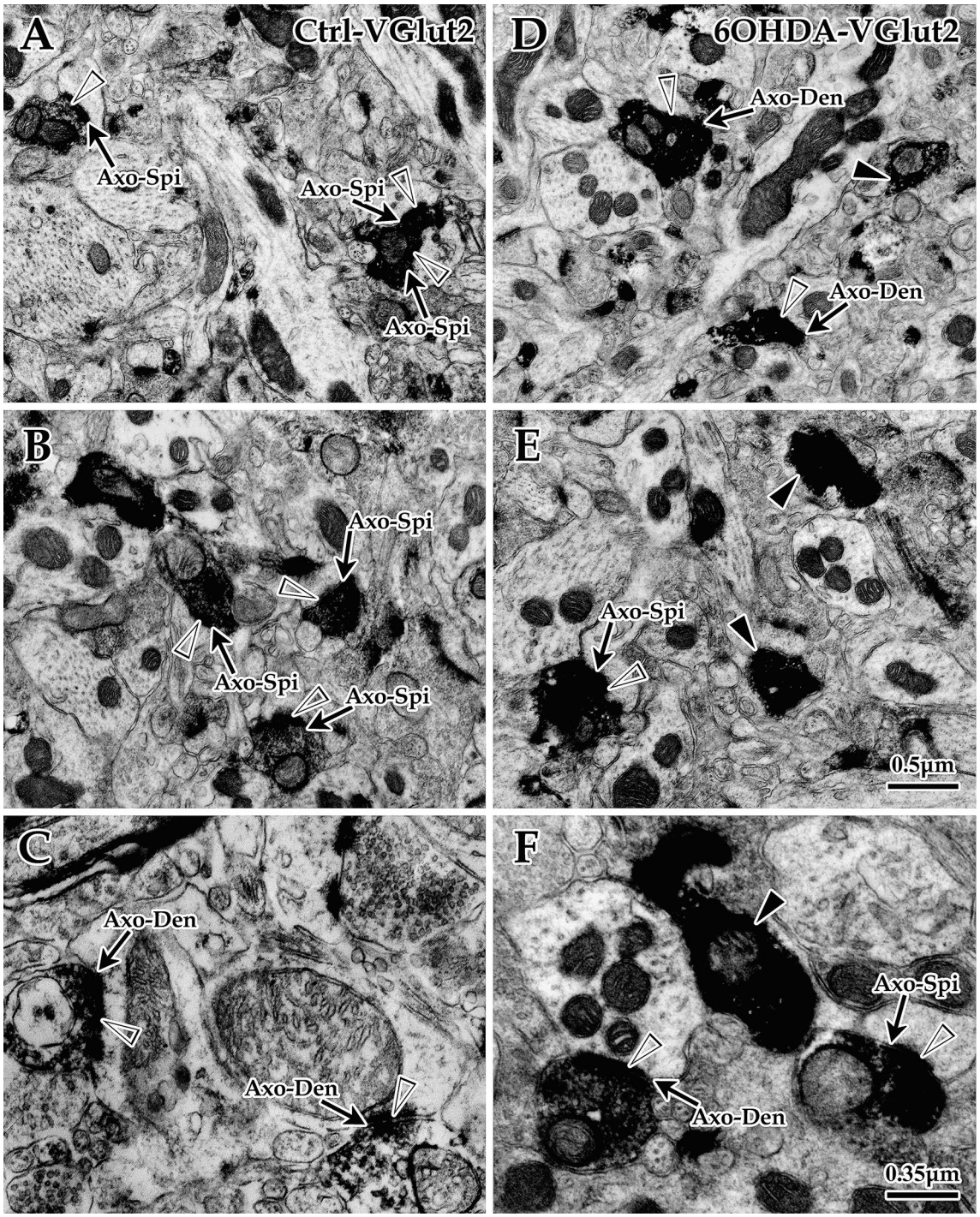

Fig. 3 Immuno-EM exploration for morphological changes of intrastriatal VGlut2+ synapses after 6OHDA-induced DA-depletion. VGlut2+ terminals are shown in the control group (**a**–**c**) and the 6OHDA group (**d**–**f**). The black arrow (→) represents VGlut2 immunolabeled excitatory synapses. White arrowheads (open triangle) point to PSD of asymmetric synapses. The black arrowheads (filled triangle) indicate VGlut2+ terminals without synapse formation. *Axo-Spi* axospinous synapses, *Axo-Den* axodendritic synapses. **a, b, d, e** were the same magnification and scale bar = 0.5 μm. **c, f** were the same magnification and scale bar = 0.5 μm

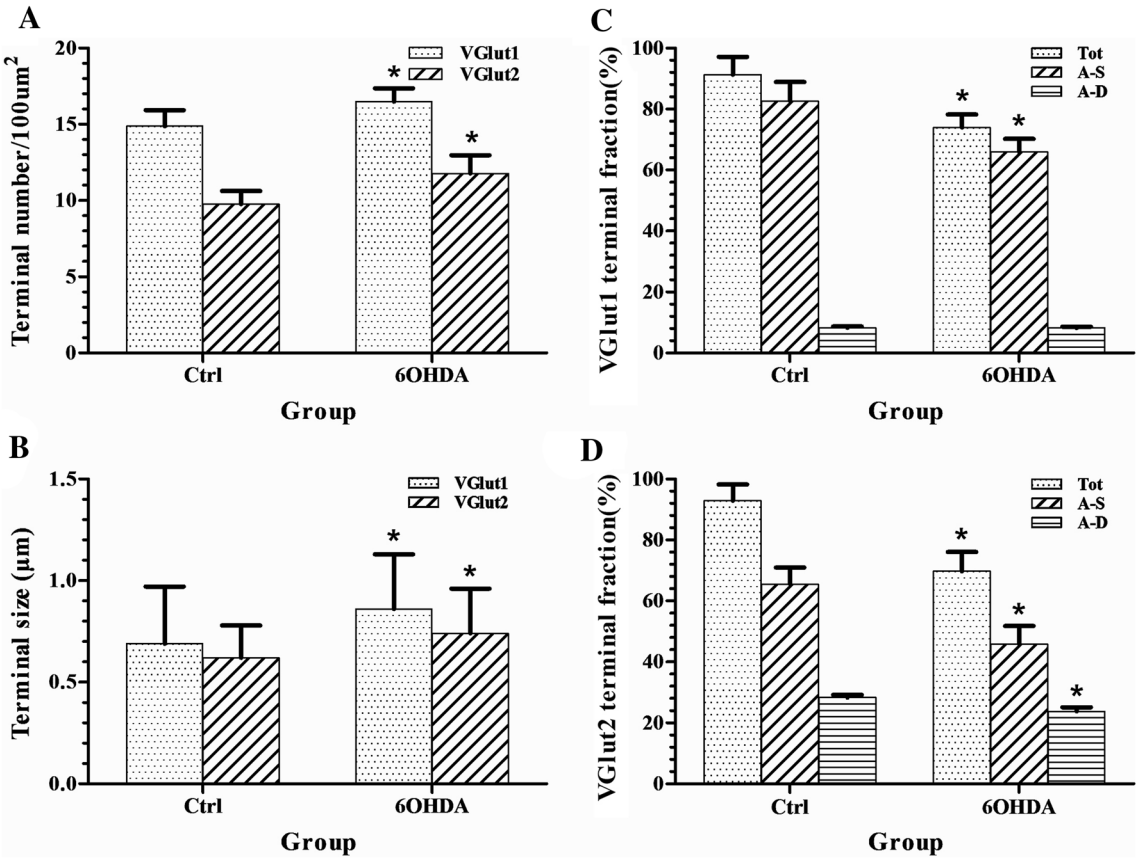

Fig. 4 Effects of 6OHDA-induced DA-depletion on morphology of VGlut1+ and VGlut2+ terminals and synapses. Histogram **a** shows the comparison of VGlut1+ and VGlut2+ terminal densities between the control group and the 6OHDA group for EM data, indicating that both VGlut1+ and VGlut2+ terminal densities increased in 6OHDA groups compared to their control groups. Histogram **b** shows comparison of VGlut1 and VGlut2+ terminal sizes between the control and the 6OHDA group, and indicating that both VGlut1 and VGlut2+ terminal sizes were bigger in the 6OHDA group compared with the control group. Histogram **c** shows terminal fractions of VGlut1+ terminals, revealing that both the total terminal fraction and axospinous rate of VGlut1+ were significantly reduced, but there was no obvious change in the axodendritic terminal fraction. Histogram **d** shows that total terminal fraction, axospinous terminal fraction and axodendritic terminal fraction of VGlut2+ were significantly lower in the 6OHDA group than the control group. *Tot* total terminal fraction; *A–S* axospinous terminal fraction; *A–D* axodendritic terminal fraction. *$P < 0.05$, comparison between the control and the 6OHDA group

6OHDA group (1.00 ± 0.08) than that in the control group (0.75 ± 0.04, $P < 0.05$; Fig. 5).

Discussion

Morphological Changes of Corticostriatal and Thalamostriatal Glutamatergic Afferents in PD

It is well known that degeneration of the dopaminergic neurons in SNc is the main pathological mechanism of PD. The loss of dopaminergic neurons result in striatal DA-depletion and induces an imbalance between excitatory and inhibitory inputs of MSNs, ultimately causing the dysfunction and remodeling of striatal neurons [9, 58, 59]. DA-depletion induces significant dendrite pruning and spine loss in striatal neurons [7, 27–29, 60]. In line with these results, we found that both VGlut1+ and VGlut2+ excitatory synapses were significantly reduced in 6OHDA-treated rats [4, 31, 44]. Recent studies have also found that VGlut1+ and VGlut2+ synapses were down-regulated in the striatum of parkinsonian rats and monkeys [24, 44]. Nevertheless, the present western blotting results showed that VGlut1 and VGlut2 protein expression levels were significantly increased in the 6OHDA group, which is in accordance with studies examining the striatum of PD monkeys and the putamen of PD patients [31, 38]. According to the EM observation, except for terminals located on spines or dendrites, there were many terminals with no overt PSD. In the present study, we counted all VGlut1+ and VGlut2+ terminals regardless of whether they formed synapses or not. Even though the density of synapses were decreased, present results showed that the densities of VGlut1+ and VGlut2+ terminals were

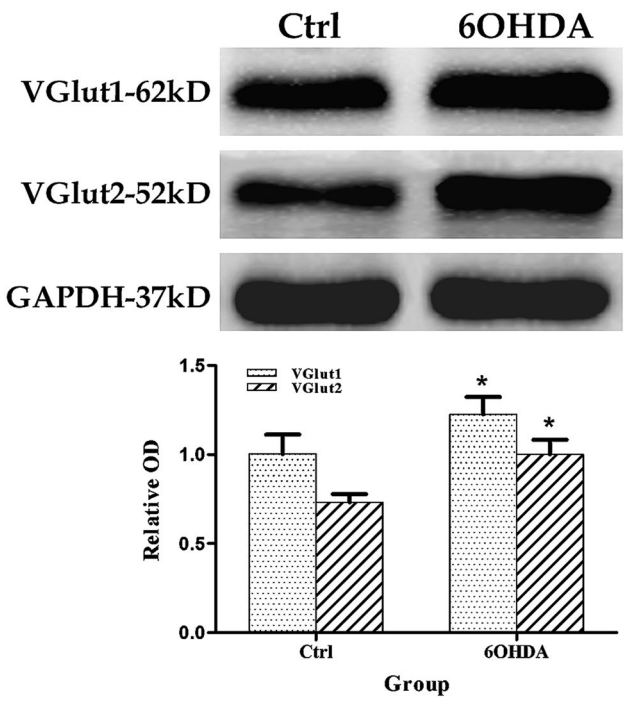

Fig. 5 Effects of striatal DA-depletion on VGlut1 and VGlut2 protein levels. Western blotting showed a prominent band at 60 kDa corresponding to the molecular weight of VGlut1 and VGlut2. Both VGlut1 and VGlut2 protein levels increased significantly in the 6OHDA group in comparison with the control group. $*P < 0.05$, comparison between the control and the 6OHDA groups

significantly increased. Thus, the total terminal fraction of VGluts+ terminals significantly decreased in rat models of PD. DA-depletion induced by 6OHDA resulted in the significant loss of axospinous synapses for both VGlut1+ and VGlut2+ terminals. However, the VGlut1+ axodendritic terminal fraction did not change and VGlut2+ axodendritic terminal fraction changed only slightly. The reduction in VGlut1+ and VGlut2+ total terminal fractions was mainly caused by loss of axospinous synapses [4]. The present study further suggested that the loss of spines after 6-OHDA lesions was accompanied by a loss of axospinous synapses rather than a movement of terminals from the spines to other postsynaptic targets [29]. We cannot completely rule out the possibility that some terminals that failed to form synapses in our EM observation could have been connect to postsynaptic structures in adjacent slices, but the mutual authentication of LM and EM results can accurately reflect the trends of observed for these terminals. Three-dimensional (3D) EM may be a more appropriate means of resolve this defect [24, 61]. Moreover, researchers have observed bilateral changes in the protein expression levels of both VGluts in the striatum of hemiparkinson rats indicative of time-dependent changes of in VGluts+ terminals [38]. Thus, more studies were needed to verify whether the size and density increase of glutamatergic terminals after 6OHDA treatment were adaptive, regenerative spouting efforts which might even diminish below control in the long run.

Transmission of VGlut1+ and VGlut2+ Excitatory Synapses Increased After 6OHDA-Induced DA-Depletion

In accordance with previous studies, we found that excitatory synapses decreased in the striatum of 6OHDA-induced PD rat models [29]. However, DA deficiency in the striatum has been shown to increase the release of glutamate in the striatum of PD rat models [62]. In line with this observation, our results showed that the size and the protein expression levels of VGlut1+ and VGlut2+ terminals were noticeably increased. Furthermore, both VGlut1+ and VGlut2+ axospinous synapses had larger spine volume, larger PSD, increased PSD perforations, and larger presynaptic terminals in the PD condition [63, 64]. Similar changes were found in the striatum of MPTP-treated monkeys by 3D EM reconstruction [24]. These morphological changes were consistent with the enhancement of synaptic function [65]. Consistent with these morphological changes, spontaneous activity in spiny neurons increased significantly and the cortically evoked excitatory synaptic transmission is facilitated after DA denervation [66]. Moreover, the synaptic activity increase may help to explain the increased intrinsic excitability of both direct and indirect pathway neurons in PD mice [67, 68]. Additionally, the function of VGluts terminals without overt synapse formation also enlarged after DA terminal depletion. We hypothesized that VGluts terminals formed synapses and those that without overt PSD came from the same region of cortex or thalamus, thus they went through similar changes of morphology and protein expression levels after 6OHDA treatment. A previous study indicated that unilateral lesion of dopaminergic neurons induced a significant increase of glutamatergic neurotransmission in bilateral striatum, which may mediated via a nigro-thalamo-cortico-striatal pathway with bilateral projections to striatum [62]. However, the loss of spines and asymmetric synapses occurred only in the lesioned striatum of 6OHDA-induced unilateral DA denervation [29, 60]. Thus, further studies are needed to characterize the morphological and pathological changes in the contralateral striatum of rats after unilateral 6-OHDA lesion. Above all, the spines were pruned and the densities of corticostriatal and thalamostriatal synapses were reduced after DA-depletion, but the residual synaptic strength was increased [4].

In conclusion, DA-depletion results in significant morphological changes to the corticostriatal and thalamostriatal input systems: the density and size of glutamatergic terminals increased significantly with 6OHDA treatment,

but with an obvious decrease in their terminal fractions. Present results suggest that 6OHDA-induced DA-depletion affects corticostriatal and thalamostriatal glutamatergic synaptic inputs, which is involved in the pathological process of striatal neuron injury induced by DA-depletion.

Acknowledgements This work was supported by the National Natural Science Foundation of China (Grant No. 81471288), and by the National Key R&D Program of China (Grant No. 2017YFA0104704).

Compliance with Ethical Standards

Conflict of interest The authors declare that they have no conflict of interest.

Ethical approval All animal experiments were performed according to the National Institutes of Health Guide for the Care and Use of Laboratory Animals conducted and approved by the Animal Care and Use Committee of Sun Yat-sen University.

References

1. Zhai S, Tanimura A, Graves SM, Shen W, Surmeier DJ (2018) Striatal synapses, circuits, and Parkinson's disease. Curr Opin Neurobiol 48:9–16
2. Albin RL, Young AB, Penney JB (1989) The functional anatomy of basal ganglia disorders. Trends Neurosci 12:366–375
3. Koos T, Tepper JM (1999) Inhibitory control of neostriatal projection neurons by GABAergic interneurons. Nat Neurosci 2:467–472
4. Fieblinger T, Graves SM, Sebel LE, Alcacer C, Plotkin JL, Gertler TS, Chan CS, Heiman M, Greengard P, Cenci MA, Surmeier DJ (2014) Cell type-specific plasticity of striatal projection neurons in parkinsonism and L-DOPA-induced dyskinesia. Nat Commun 5:5316
5. Taverna S, Ilijic E, Surmeier DJ (2008) Recurrent collateral connections of striatal medium spiny neurons are disrupted in models of Parkinson's disease. J Neurosci 28:5504–5512
6. Surmeier DJ, Plotkin J, Shen W (2009) Dopamine and synaptic plasticity in dorsal striatal circuits controlling action selection. Curr Opin Neurobiol 19:621–628
7. Ingham CA, Hood SH, Arbuthnott GW (1989) Spine density on neostriatal neurones changes with 6-hydroxydopamine lesions and with age. Brain Res 503:334–338
8. Gerfen CR, Surmeier DJ (2011) Modulation of striatal projection systems by dopamine. Annu Rev Neurosci 34:441–466
9. Deutch AY, Colbran RJ, Winder DJ (2007) Striatal plasticity and medium spiny neuron dendritic remodeling in parkinsonism. Parkinsonism Relat Disord 13(Suppl 3):S251–S258
10. Smith Y, Bevan MD, Shink E, Bolam JP (1998) Microcircuitry of the direct and indirect pathways of the basal ganglia. Neuroscience 86:353–387
11. Wickens JR, Budd CS, Hyland BI, Arbuthnott GW (2007) Striatal contributions to reward and decision making: making sense of regional variations in a reiterated processing matrix. Ann NY Acad Sci 1104:192–212
12. Deutch AY (2006) Striatal plasticity in parkinsonism: dystrophic changes in medium spiny neurons and progression in Parkinson's disease. J Neural Transm Suppl 70:67–70
13. Stephens B, Mueller AJ, Shering AF, Hood SH, Taggart P, Arbuthnott GW, Bell JE, Kilford L, Kingsbury AE, Daniel SE, Ingham CA (2005) Evidence of a breakdown of corticostriatal connections in Parkinson's disease. Neuroscience 132:741–754
14. Smith Y, Galvan A, Ellender TJ, Doig N, Villalba RM, Huerta-Ocampo I, Wichmann T, Bolam JP (2014) The thalamostriatal system in normal and diseased states. Front Syst Neurosci 8:5
15. Smith Y, Raju D, Nanda B, Pare JF, Galvan A, Wichmann T (2009) The thalamostriatal systems: anatomical and functional organization in normal and parkinsonian states. Brain Res Bull 78:60–68
16. Kreitzer AC (2009) Physiology and pharmacology of striatal neurons. Annu Rev Neurosci 32:127–147
17. Surmeier DJ, Ding J, Day M, Wang Z, Shen W (2007) D1 and D2 dopamine-receptor modulation of striatal glutamatergic signaling in striatal medium spiny neurons. Trends Neurosci 30:228–235
18. Lacey CJ, Boyes J, Gerlach O, Chen L, Magill PJ, Bolam JP (2005) GABA(B) receptors at glutamatergic synapses in the rat striatum. Neuroscience 136:1083–1095
19. Raju DV, Shah DJ, Wright TM, Hall RA, Smith Y (2006) Differential synaptology of vGluT2-containing thalamostriatal afferents between the patch and matrix compartments in rats. J Comp Neurol 499:231–243
20. Mythri RB, Venkateshappa C, Harish G, Mahadevan A, Muthane UB, Yasha TC, Srinivas BM, Shankar SK (2011) Evaluation of markers of oxidative stress, antioxidant function and astrocytic proliferation in the striatum and frontal cortex of Parkinson's disease brains. Neurochem Res 36:1452–1463
21. Hoehn MM, Yahr MD (1967) Parkinsonism: onset, progression and mortality. Neurology 17:427–442
22. Venkateshappa C, Harish G, Mythri RB, Mahadevan A, Bharath MM, Shankar SK (2012) Increased oxidative damage and decreased antioxidant function in aging human substantia nigra compared to striatum: implications for Parkinson's disease. Neurochem Res 37:358–369
23. Calabresi P, Picconi B, Tozzi A, Filippo MD (2007) Dopamine-mediated regulation of corticostriatal synaptic plasticity. Trends Neurosci 30:211–219
24. Villalba RM, Smith Y (2011) Differential structural plasticity of corticostriatal and thalamostriatal axo-spinous synapses in MPTP-treated Parkinsonian monkeys. J Comp Neurol 519:989–1005
25. Jing X, Wei X, Ren M, Wang L, Zhang X, Lou H (2016) Neuroprotective effects of tanshinone I against 6-OHDA-induced oxidative stress in cellular and mouse model of Parkinson's disease through upregulating Nrf2. Neurochem Res 41:779–786
26. Jia Y, Mo SJ, Feng QQ, Zhan ML, OuYang LS, Chen JC, Ma YX, Wu JJ, Lei WL (2014) EPO-dependent activation of PI3K/Akt/FoxO3a signalling mediates neuroprotection in in vitro and in vivo models of Parkinson's disease. J Mol Neurosci 53:117–124
27. Villalba RM, Lee H, Smith Y (2009) Dopaminergic denervation and spine loss in the striatum of MPTP-treated monkeys. Exp Neurol 215:220–227
28. Zaja-Milatovic S, Milatovic D, Schantz AM, Zhang J, Montine KS, Samii A, Deutch AY, Montine TJ (2005) Dendritic degeneration in neostriatal medium spiny neurons in Parkinson disease. Neurology 64:545–547
29. Ingham CA, Hood SH, Taggart P, Arbuthnott GW (1998) Plasticity of synapses in the rat neostriatum after unilateral lesion of the nigrostriatal dopaminergic pathway. J Neurosci 18:4732–4743
30. McNeill TH, Brown SA, Rafols JA, Shoulson I (1988) Atrophy of medium spiny I striatal dendrites in advanced Parkinson's disease. Brain Res 455:148–152
31. Raju DV, Ahern TH, Shah DJ, Wright TM, Standaert DG, Hall RA, Smith Y (2008) Differential synaptic plasticity of the corticostriatal and thalamostriatal systems in an MPTP-treated monkey model of parkinsonism. Eur J Neurosci 27:1647–1658

32. Villalba RM, Smith Y (2013) Differential striatal spine pathology in Parkinson's disease and cocaine addiction: a key role of dopamine? Neuroscience 251:2–20
33. Villalba RM, Wichmann T, Smith Y (2014) Neuronal loss in the caudal intralaminar thalamic nuclei in a primate model of Parkinson's disease. Brain Struct Funct 219:381–394
34. Smith Y, Wichmann T, DeLong MR (2014) Corticostriatal and mesocortical dopamine systems: do species differences matter? Nat Rev Neurosci 15:63
35. Halliday GM (2009) Thalamic changes in Parkinson's disease. Parkinsonism Relat Disord 15(Suppl 3):S152–S155
36. Aymerich MS, Barroso-Chinea P, Perez-Manso M, Munoz-Patino AM, Moreno-Igoa M, Gonzalez-Hernandez T, Lanciego JL (2006) Consequences of unilateral nigrostriatal denervation on the thalamostriatal pathway in rats. Eur J Neurosci 23:2099–2108
37. Henderson JM, Schleimer SB, Allbutt H, Dabholkar V, Abela D, Jovic J, Quinlivan M (2005) Behavioural effects of parafascicular thalamic lesions in an animal model of parkinsonism. Behav Brain Res 162:222–232
38. Massie A, Schallier A, Vermoesen K, Arckens L, Michotte Y (2010) Biphasic and bilateral changes in striatal VGLUT1 and 2 protein expression in hemi-Parkinson rats. Neurochem Int 57:111–118
39. Kusnoor SV, Bubser M, Deutch AY (2012) The effects of nigrostriatal dopamine depletion on the thalamic parafascicular nucleus. Brain Res 1446:46–55
40. Kashani A, Betancur C, Giros B, Hirsch E, El MS (2007) Altered expression of vesicular glutamate transporters VGLUT1 and VGLUT2 in Parkinson disease. Neurobiol Aging 28:568–578
41. Marin C, Bonastre M, Aguilar E, Jimenez A (2011) The metabotropic glutamate receptor antagonist 2-methyl-6-(phenylethynyl) pyridine decreases striatal VGlut2 expression in association with an attenuation of L-DOPA-induced dyskinesias. Synapse 65:1080–1086
42. Villalba RM, Mathai A, Smith Y (2015) Morphological changes of glutamatergic synapses in animal models of Parkinson's disease. Front Neuroanat 9:117
43. Villalba RM, Smith Y (2018) Loss and remodeling of striatal dendritic spines in Parkinson's disease: from homeostasis to maladaptive plasticity? J Neural Transm (Vienna) 125:431–447
44. Zhang Y, Meredith GE, Mendoza-Elias N, Rademacher DJ, Tseng KY, Steece-Collier K (2013) Aberrant restoration of spines and their synapses in L-DOPA-induced dyskinesia: involvement of corticostriatal but not thalamostriatal synapses. J Neurosci 33:11655–11667
45. Ungerstedt U, Arbuthnott GW (1970) Quantitative recording of rotational behavior in rats after 6-hydroxy-dopamine lesions of the nigrostriatal dopamine system. Brain Res 24:485–493
46. Hefti F, Melamed E, Wurtman RJ (1980) Partial lesions of the dopaminergic nigrostriatal system in rat brain: biochemical characterization. Brain Res 195:123–137
47. Ma Y, Zhan M, OuYang L, Li Y, Chen S, Wu J, Chen J, Luo C, Lei W (2014) The effects of unilateral 6-OHDA lesion in medial forebrain bundle on the motor, cognitive dysfunctions and vulnerability of different striatal interneuron types in rats. Behav Brain Res 266:37–45
48. Zheng X, Wu J, Zhu Y, Chen S, Chen Z, Chen T, Huang Z, Wei J, Li Y, Lei W (2018) A comparative study for striatal-direct and -indirect pathway neurons to DA depletion-induced lesion in a PD rat model. Neurochem Int 118:14–22
49. Yuan H, Sarre S, Ebinger G, Michotte Y (2005) Histological, behavioural and neurochemical evaluation of medial forebrain bundle and striatal 6-OHDA lesions as rat models of Parkinson's disease. J Neurosci Methods 144:35–45
50. Paxinos G, Watson C (1986) The rat brain in stereotaxic coordinates. Elsevier, San Diego
51. Gittis AH, Kreitzer AC (2012) Striatal microcircuitry and movement disorders. Trends Neurosci 35:557–564
52. Mu S, OuYang L, Liu B, Zhu Y, Li K, Zhan M, Liu Z, Jia Y, Lei W (2011) Protective effect of melatonin on 3-NP induced striatal interneuron injury in rats. Neurochem Int 59:224–234
53. Mu S, Lin E, Liu B, Ma Y, OuYang L, Li Y, Chen S, Zhang J, Lei W (2014) Melatonin reduces projection neuronal injury induced by 3-nitropropionic acid in the rat striatum. Neurodegener Dis 14:139–150
54. Deng YP, Wong T, Bricker-Anthony C, Deng B, Reiner A (2013) Loss of corticostriatal and thalamostriatal synaptic terminals precedes striatal projection neuron pathology in heterozygous Q140 Huntington's disease mice. Neurobiol Dis 60:89–107
55. Lei W, Deng Y, Liu B, Mu S, Guley NM, Wong T, Reiner A (2013) Confocal laser scanning microscopy and ultrastructural study of VGLUT2 thalamic input to striatal projection neurons in rats. J Comp Neurol 521:1354–1377
56. Lei W, Jiao Y, Del MN, Reiner A (2004) Evidence for differential cortical input to direct pathway versus indirect pathway striatal projection neurons in rats. J Neurosci 24:8289–8299
57. Hisano S, Hoshi K, Ikeda Y, Maruyama D, Kanemoto M, Ichijo H, Kojima I, Takeda J, Nogami H (2000) Regional expression of a gene encoding a neuron-specific Na(+)-dependent inorganic phosphate cotransporter (DNPI) in the rat forebrain. Mol Brain Res 83:34–43
58. Segal M, Andersen P (2000) Dendritic spines shaped by synaptic activity. Curr Opin Neurobiol 10:582–586
59. Shen W, Flajolet M, Greengard P, Surmeier DJ (2008) Dichotomous dopaminergic control of striatal synaptic plasticity. Science 321:848–851
60. Day M, Wang Z, Ding J, An X, Ingham CA, Shering AF, Wokosin D, Ilijic E, Sun Z, Sampson AR, Mugnaini E, Deutch AY, Sesack SR, Arbuthnott GW, Surmeier DJ (2006) Selective elimination of glutamatergic synapses on striatopallidal neurons in Parkinson disease models. Nat Neurosci 9:251–259
61. Smith Y, Villalba RM, Raju DV (2009) Striatal spine plasticity in Parkinson's disease: pathological or not? Parkinsonism Relat Disord 15(Suppl 3):S156–S161
62. Lindefors N, Ungerstedt U (1990) Bilateral regulation of glutamate tissue and extracellular levels in caudate-putamen by midbrain dopamine neurons. Neurosci Lett 115:248–252
63. Meshul CK, Allen C (2000) Haloperidol reverses the changes in striatal glutamatergic immunolabeling following a 6-OHDA lesion. Synapse 36:129–142
64. Harris KM, Kater SB (1994) Dendritic spines: cellular specializations imparting both stability and flexibility to synaptic function. Annu Rev Neurosci 17:341–371
65. Lisman JE, Harris KM (1993) Quantal analysis and synaptic anatomy—integrating two views of hippocampal plasticity. Trends Neurosci 16:141–147
66. Pang Z, Ling GY, Gajendiran M, Xu ZC (2001) Enhanced excitatory synaptic transmission in spiny neurons of rat striatum after unilateral dopamine denervation. Neurosci Lett 308:201–205
67. Toy WA, Petzinger GM, Leyshon BJ, Akopian GK, Walsh JP, Hoffman MV, Vuckovic MG, Jakowec MW (2014) Treadmill exercise reverses dendritic spine loss in direct and indirect striatal medium spiny neurons in the 1-methyl-4-phenyl-1,2,3,6-tetrahydropyridine (MPTP) mouse model of Parkinson's disease. Neurobiol Dis 63:201–209
68. Suarez LM, Solis O, Aguado C, Lujan R, Moratalla R (2016) L-DOPA oppositely regulates synaptic strength and spine morphology in D1 and D2 striatal projection neurons in dyskinesia. Cereb Cortex 26:4253–4264